International Journal of Coal Science & Technology (2023) 10:88
https://doi.org/10.1007/s40789-023-00621-5

RESEARCH

Microstructure and adhesion force of dust on soil pavement in open-pit mine

Jiuzhu Wang[1,2] · Cuifeng Du[1,2] · Yuan Wang[1,2] · Zheng Chen[1,2]

Received: 24 December 2022 / Revised: 13 March 2023 / Accepted: 3 August 2023

Abstract
The microstructure and adhesion force between dust particles determine the dust starting and migration to a certain extent. By use of scanning electron microscopy, the BET method, and the abruption technique, the microstructure and adhesion force of dust on the soil pavement of an open-pit mine were examined. The results indicate that the dust shape of soil pavement is mainly irregular quadrilateral, pentagonal and circular. The adhesion of dust particles in soil pavement reduces as particle size and temperature increase. When the particle size grows from 22 to 30 μm and the ambient temperature rises from 25 to 30 ℃, the adhesion force of dust particles in soil pavement drops dramatically. The adhesion force of dust particles in the soil pavement of open-pit mine increases as environmental humidity and pressure rise. When the environmental humidity exceeds 70% and pressure exceeds 24.79 kPa, the adhesion of dust particles increases dramatically. On the basis of the multiple regression method, a prediction model for the dust adhesion force of open-pit mines' soil pavement has been developed. However, its accuracy needs to be further enhanced.

Keywords Adhesion force · Soil pavement · Dust · Microstructure · Influence factor

1 Introduction

With high transportation efficiency and flexibility, automobile transportation has become the main transportation mode for open-pit mines. The road surface of the open-pit mine generates powder due to the rolling and bumping of mine cars, resulting in a large amount of floating dust accumulating on the road surface. Therefore, road dust is one of the essential sources of dust pollution in mines. The microstructure and adhesive force of dust determine the generation and diffusion of dust to a certain extent.

The microstructure of dust can be analyzed by scanning electron microscope (Jin et al. 2021), some scholars also proposed to combine it with Image J software (Mazzoli and Favoni 2012). At present, scholars have mostly studied the microscopic characteristics of dust on urban roads (Bucko et al. 2011; Wiseman et al. 2021), tunnels (Klockner et al. 2021) and industrial roads (Jayarathne et al. 2019; Ramirez et al. 2020), but rarely on mine dust, especially on soil pavement. Barone et al. (2019) used light-scattering theories to determine the particle size of irregular particles, and analyzed the composition and morphology of coal dust. Qian et al. (2020) analyzed the micromorphology and microstructure of coal mine dust after explosion from the qualitative and quantitative point of view, and divided the dust after explosion into four types, the dust with large particle size is in the shape of regular spherical and ellipsoidal particles. Liu et al. (2021) analyzed the trace elements in the road dust around coal-fired power plant through cluster analysis, isotope monitoring, and XPS observation.

The adhesion between particles mainly includes van der Waals force, capillary force and electrostatic force (Isaifan et al. 2019). The main methods for testing adhesion force include atomic force microscopy (Jaiswal et al. 2009), centrifuge method (Nguyen et al. 2010), electrostatic detachment method (Hu et al. 2008) and vibration method (Ripperger and Hein 2005). Nguyen et al. (2010) used atomic force microscopy and centrifugation to measure the adhesion characteristics between particles because of the great variation in the measurement results of atomic force microscopy. Even

✉ Cuifeng Du
ducuifeng@126.com

[1] College of Civil and Resource Engineering, University of Science and Technology Beijing, Beijing 100083, China

[2] State Key Laboratory of High-Efficient Mining and Safety of Metal Mines University of Science and Technology Beijing, Ministry of Education, Beijing 100083, China

Published online: 09 December 2023

for the same particles, particle shape and surface topography will affect the measurement. Hence, many scholars have proposed new methods for measuring adhesion force. Zafar et al. (2014) has developed a rapid method for measuring adhesion forces by attaching particles to a substrate, dropping the substrate at a certain height onto a bottom-mounted plug, forcing the granules off the substrate, and then using Newton's second law of motion to estimate the separation force. Karde et al. (2017) utilized the tensile strength measurements to estimate the adhesion force for different consolidation stresses and wet conditions to estimate the change in adhesion between corn starch granules. Deng et al. (2021) adopted a novel mechanical surface energy tester to measure the particle adhesions of cohesive powders. Zhang et al. (2020) measured the interaction force between particle and air bubble/water droplet through a micromechanical tester. The test method for dust adhesion force can be referred to Chinese GB/T 16913-2008. In the past, Shi et al. (2017) conducted a study on the effect of denitrification and flue gas Waste Heat Recovery System on the adhesion force of ash particles. Although the test methods of particle adhesion forces are relatively mature, there are few reports on dust adhesion force testing of soil pavements in open-pit mines.

In conclusion, the microstructure of mine dust has been widely discussed, but research on the microstructure and adhesion force of soil pavement dust is lacking. The adhesion force of open-pit mine dust not only determines the dust generation and migration to a certain extent, but also can be used as an evaluation index for the development and selection of chemical dust suppressants. Thus, in this study, the dust microstructure and adhesion force of mine soil pavement are explored in depth to provide a theoretical basis for dust mechanism analysis and dust suppression of soil pavement in open-pit mines.

2 Description of experiments

2.1 Sample preparation

The dust samples were taken from an iron mine soil pavement with a brush. According to AP-42 of the United States, 5–10 kg samples were randomly selected from three locations of the road for microstructure analysis since the road did not exceed 4.8 km. After collecting the samples, the silt content and water content of the roads were determined to be 11.63% and 0.051%, respectively. In addition, the samples were screened by standard sieves to remove particles larger than 80 mesh to analyze the adhesion of dust on the soil pavement. As can be observed in Fig. 1, dusts with particle size of 180, 120 and 75 μm respectively account for 53.49%, 21.6% and 14.33% of the dust on the soil pavement of open-pit mine.

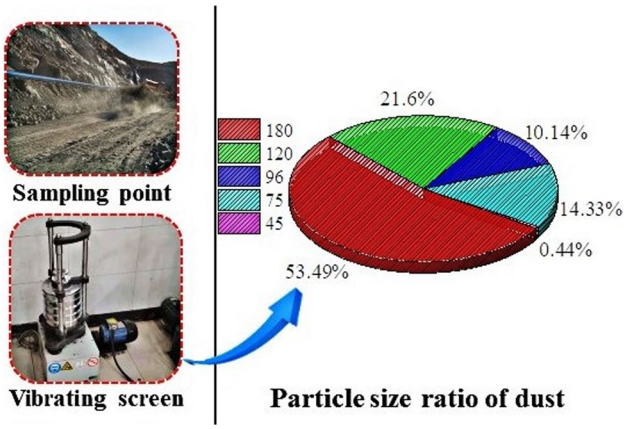

Fig. 1 Sampling position and particle size ratio of dust

2.2 Experimental methods

(1) Microscopic morphology test method. The microscopic morphology and composition of dust of mine soil pavement were analyzed by ZEISS microscope. Since dry dust is not electrically charged, it can destroy the electron beam. In order to avoid this problem, the dust was installed on a carbon band, which was then sprayed to improve its electrical conductivity. The scanning electron microscope images of dust were taken at an accelerating voltage of 10–12 kV and an observation distance of 10–14 mm.

(2) Pore structure test method. ASAP2020M was used to measure the pore structure parameters of the soil pavement particles in the open-pit mine. During the experiment, the dust samples were put into a vacuum degassing station for heating and degassing treatment under the degassing temperature of 120 ℃ for 2 h. Afterwards, the dust samples were put into liquid nitrogen bottles for testing.

(3) Adhesion test method. The adhesion of mine soil pavement dust was tested in accordance with the abruption method of GBT16913-2008. This test principle is to put the dust into the separable sleeve sample box, vibrate and fill it tightly, and then pull off the dust sample vertically on the viscosity balance. The measured vertical tensile strength of the dust sample represents the adhesion force of the dust. As a modification of the TG628A analytical balance, the test apparatus for the abruption method is shown in Fig. 2a. The device is mainly composed of an upper barrel, a lower barrel, a light measuring cylinder, a fixture and an adjustable support (GB/T 16913-2008). The diameter of the upper and lower barrels is 2 cm, and the lower barrel is cup-shaped. The upper and lower barrel can form a sample box under the action of the fixture, and then

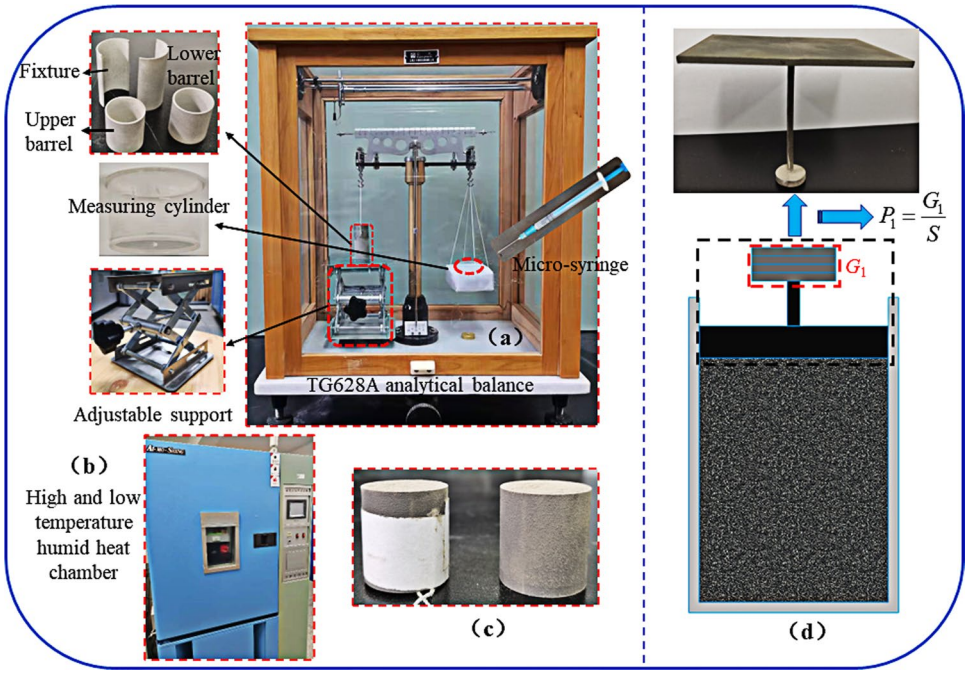

Fig. 2 Schematic diagram of experimental device

filled with dust from the open-pit mine soil pavement. The micro-syringe serves to inject water into the measuring cylinder. The temperature and humidity of dust can be controlled by a high and low temperature humid heat chamber (Fig. 2b). The sample to be measured was placed in the high and low temperature humid heat chamber for 1 h and then immediately removed for measurement. The vibration caused by water injection should be avoided during the experiment. Moreover, if a concave and convex surface was formed after fracture, the actual fracture area would be larger than that of the calculated adhesion, and thus increase the error. The qualified fracture surface is depicted in Fig. 2c. In this paper, the temperature and the humidity ranged from 25 to 40 ℃ and 30% to 90%, respectively. The pressing pressure was different weights of dust pressed into the barrel through the device (d) with conversion pressures of 12.48, 24.79, 37.45, and 49.9 kPa, respectively.

2.3 Data analysis

The analytical balance was adjusted to zero, the sample box with dust was placed on the lifting support and the adjustable support was adjusted so that the sample box was attached vertically to the left arm hook of the contact balance without force, then the fixture was removed and a few attention was paid to prevent dislocation. The light tray was hanged on the right arm of the analytical balance, and the light measuring cylinder was placed into the tray. The micro-syringe was utilized to inject water into the tray and observe the pointer. The force diagram in the abruption experiment is described in Fig. 3. The force balance can be determined by the following equations:

$$p+Gg = Wg \tag{1}$$

where p denotes the adhesion force of dust, W denotes the total weight of the dust cylinder and G denotes the total weight of dust in upper barrel and barrel.

If the pointer jumps to the left, stop water injection. At this point, the dust has been broken. The adhesion force of dust can be calculated by Eq. (2):

$$p = \frac{W - G}{S} \tag{2}$$

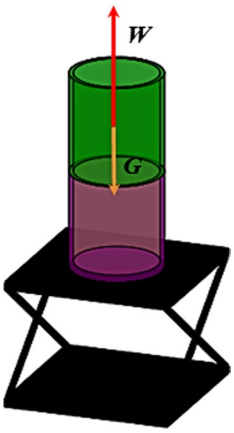

Fig. 3 Force diagram of the abruption experiment

where S denotes the area of the measuring cross-section.

Follow the above steps and methods for 3–5 consecutive measurements and calculate the average value.

3 Results and discussion

3.1 Microstructure of soil pavement dust in open-pit mine

3.1.1 Microscopic morphology and composition of soil pavement dust

The microscopic morphology of the soil pavement of the open-pit mine is shown in Fig. 4. It can be seen from the figure that the shape of dust on the open-pit road is mostly irregular, mainly irregular quadrilateral, pentagonal (Figs. 4a, b, d, e) and nearly circular (Fig. 4c).

The dust energy spectrum of soil pavement of the open-pit mine is depicted in Fig. 5. According to this figure, the main elements in the dust of the soil pavement of the open-pit mine include Si, Ca, Fe, Mg and Al, in which Al and Fe elements were likely to be emitted from automobile exhaust (Yang et al. 2019).

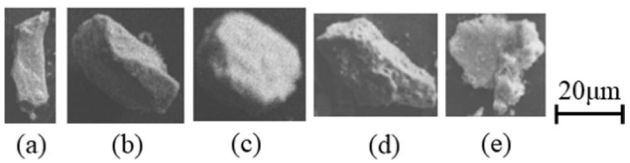

Fig. 4 Microscopic morphology of dust on soil pavement of open-pit mine: **a**–**b** Irregular quadrilateral; **c** Nearly circular; **d** Irregular pentagonal; **e** Irregular polygon

3.1.2 Dust pore structure of soil pavement in open-pit mine

The low temperature liquid nitrogen adsorption desorption curve of dust on soil pavement of open-pit mine are described in Fig. 6. When the relative pressure was less than 0.8, the adsorption curve rises slowly and not vice-versa. This mainly stems from the capillary condensation of the larger pores in the soil pavement particles, resulting in a sharp increase of the adsorption capacity. There is no inflection point in the desorption line, and the difference between the desorption line and the adsorption line is small, suggesting that the soil pavement particles in the open-pit mine are mainly composed of airtight holes closed at one end (Yan and Zhang 1979). The shape of the adsorption isotherm of the soil pavement particles of the open-pit mine shows that the adsorption isotherm of the soil pavement particles in open-pit mine belongs to type II. This also reveals that the soil pavement particles in open-pit mine have a relatively complete pore structure, which ranged from micropores to infinite pores (Chen and Tang 2001).

The specific surface area and pore volume of dust calculated from low temperature liquid nitrogen adsorption and desorption data are demonstrated in Table 1. From this table, it can be seen from that the specific surface area and the total pore volume of soil pavement dust of open-pit mine are 2.717 m^2/g and 0.024 cm^3/g, respectively.

In order to intuitively analyze the dust pore size distribution of soil pavement of an open-pit mine, the integral and differential curves of pore size were plotted using the density

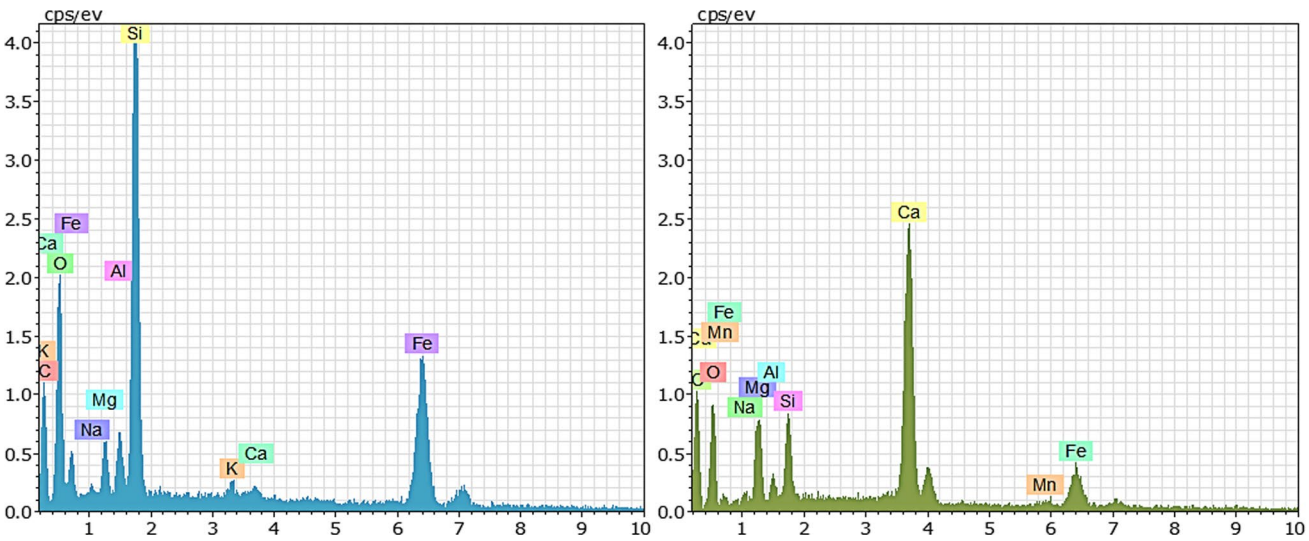

Fig. 5 Dust energy spectrum of soil pavement in open-pit mine

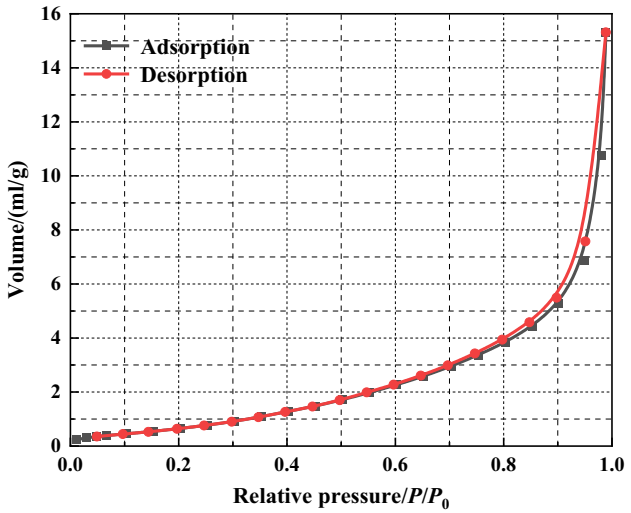

Fig. 6 Low temperature liquid nitrogen adsorption desorption curve of dust on soil pavement of open-pit mine

Table1 Structure parameters of dust pore in soil pavement of open-pit mine

Specific surface area (m^2/g)	Pore volume (cm^3/g)		
	DFT	BJH	Total pore volume
2.717	0.011	0.025	0.024

flooding theory (DFT) model (Fig. 7). It's worth noting that the dust pore size of soil pavement of open-pit mine mainly ranges from 3.47 to 25.12 nm. In addition, the most probable pore diameter is 4.54 nm, indicating that the mesopores of soil pavement dust in open-pit mine are more developed in comparison.

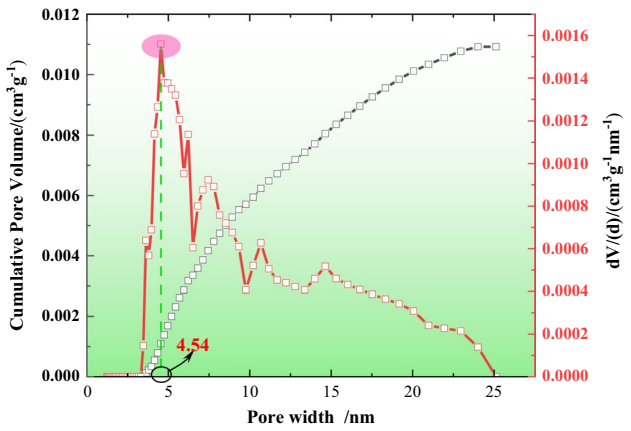

Fig.7 Pore size distribution of dust on soil pavement of open-pit mine

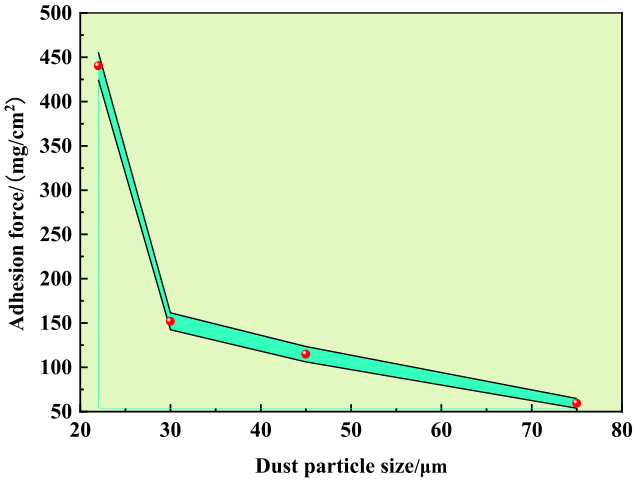

Fig. 8 Influence of particle size on dust adhesion of soil pavement

3.2 Influence of different factors on dust adhesion of soil pavement

3.2.1 Particle size

The particle size of 75, 45, 30 and 22 μm were respectively screened by 200, 325, 500 and 800 mesh standard screens to analyze the influence of particle size on dust adhesion force of soil pavement of open-pit mine. The adhesion force of full-size dust on open-pit soil pavement is 8.09 mg/cm^2. The variation trend of dust adhesion force of soil pavement of open-pit mine with different particle sizes is shown in Fig. 8. It is clear that the dust adhesion force of soil pavement gradually decreases with the increase of dust particle size. When dust particle size reached 22 μm and 30 μm, the corresponding dust adhesion force are 440.17 mg/cm^2 and 151.88 mg/cm^2. Meanwhile, the dust adhesion force of soil pavement decreases rapidly when the dust particle size increased. The possible reasons for this phenomenon are as follows: when the ambient humidity and pressure were constant, the larger the particle size of dust led to a smaller specific surface area, and the probability of dust adhesion to each other decreases, thus causing the reduction of adhesion force (Shi et al. 2017).

3.2.2 Ambient humidity

The variation trend of dust adhesion force of soil pavement with different humidity are described in Fig. 9. As can be seen from Fig. 9, the dust adhesion force increases with the increase of humidity. When the ambient humidity was less than 70%, the dust adhesion force of soil pavement is less than 310 mg/cm^2. However, the dust adhesion force

increases obviously, up to 2000 mg/cm^2 when the ambient humidity exceeded 70%. This is consistent with the results of previous studies (Isaifan et al. 2019). When the humidity increased to 70%–90%, the dust adhesion force increases rapidly. This can be attributed that the dust moisture content approximately doubles when the ambient humidity increased from 70% to 90%, and the increase of moisture content led to a rapid increase in adhesion force. In addition, the dust moisture content increases when increasing the humidity. When the environmental humidity increased from 30% to 90%, the dust moisture content of soil pavement increases from 0.099% to 1.210%, indicating that the environmental humidity imposed a significant effect on the dust moisture content in soil pavement of open-pit mine.

Dust adhesion force mainly includes van der Waals force, electrostatic force and capillary force, among which capillary force depends mainly on the surrounding environment.

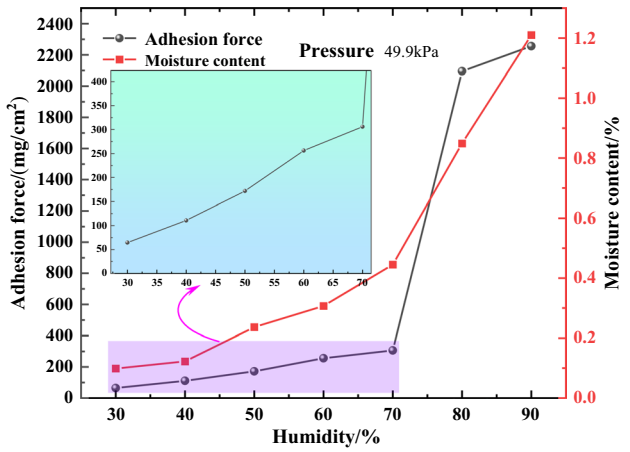

Fig. 9 Influence of environmental humidity on dust adhesion of soil pavement

Capillary force is the formation of a thin liquid film on the surface of dust in a humid environment. When the liquid film of different dust was in contact with each other, a liquid bridge would be formed because of the surface tension of the liquid film as well as the adhesion of different dusts under the action of the liquid bridge. When the humidity increased, the dust moisture content increased, and the capillary force increased, thereby increasing the dust adhesion force (Jones et al. 2002).

3.2.3 Pressure

The change trend of dust adhesion force of soil pavement of open-pit mine with pressure is shown in Fig. 10a. As can be observed from this figure, the dust adhesion force increased with the increase of pressure. When the pressure was less than 24.79 kPa, the change trend of dust adhesion force is small. Nevertheless, the increase of dust adhesion force was large when the pressure was 37.45–49.9 kPa. At the same time, the dust adhesion force increased from 48.15 mg/cm^2 to about 100 mg/cm^2. This can be explained by that the dust is mostly irregular in shape based on the analysis of dust microscopic morphology. Moreover, when the pressure increased, the dust would overcome the internal force of the dust and deform. The deformed dust increased the contact area between the dust and thus increased the adhesion force of the dust (Fig. 10b).

3.2.4 Temperature

The variation trend of dust adhesion force and dust moisture content on soil pavement of open-pit mine with temperature are described in Fig. 11. Notably, the dust adhesion force and moisture content gradually decrease and stabilize as the temperature increased. As the temperature increased from 25 to

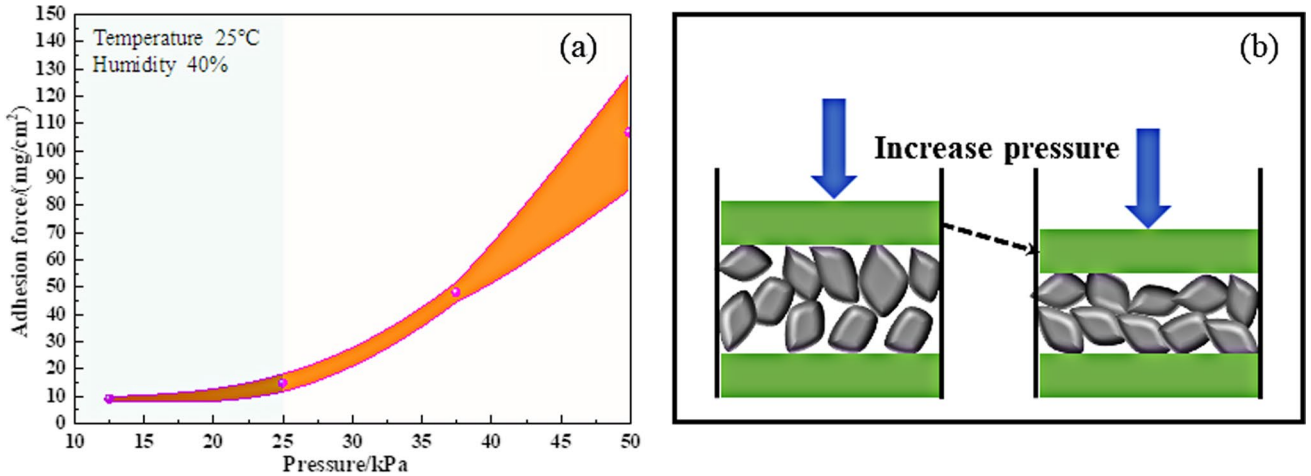

Fig. 10 Influence of pressure on dust adhesion of soil pavement: **a** Adhesion force; **b** Schematic diagram of contact between particles

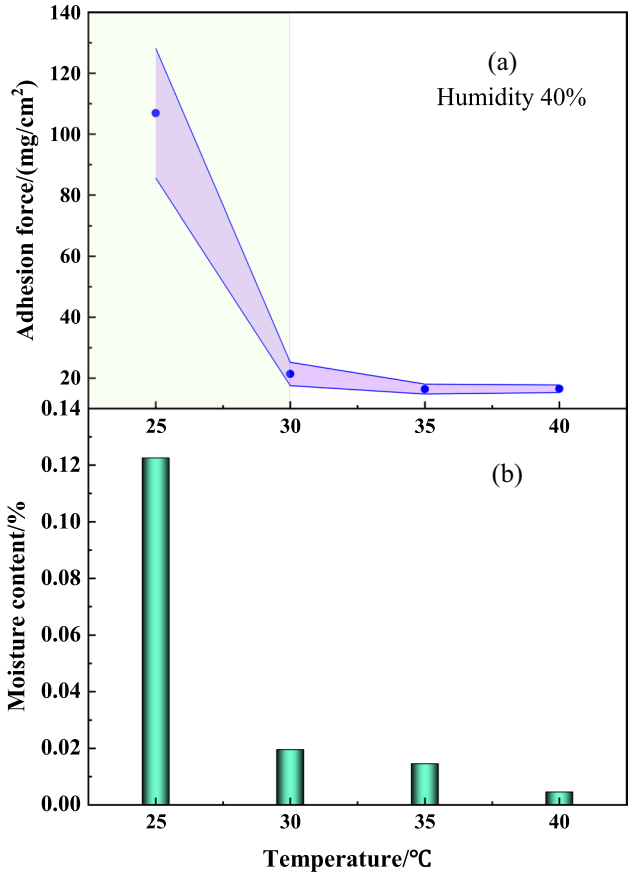

Fig. 11 Influence of temperature on dust adhesion of soil pavement: **a** Adhesion force; **b** Moisture content

30 ℃, the dust adhesion force plummets. The reason may be that the increase in temperature caused the dust moisture content to decrease from 0.12% to 0.02%, and the decrease of moisture content led to a decrease of capillary force between dust and the reduction of adhesion force. The dust adhesion decreased slightly and tended to be stable when the temperature was between 30 and 40 ℃. At this time, the dust moisture content is small and close to each other (Fig. 11b). Therefore, changing temperature imposed little influence on the dust adhesion force.

3.3 Establishment of the dust adhesion force prediction model

In order to establish the relationship between the dust adhesion force of open-pit mine soil pavement and each factor, the variation of dust adhesion force under temperature, humidity, particle size and pressure was obtained by using orthogonal test method. The factor setting table of the orthogonal experiment is shown in the Table 2.

In accordance with Table 2, the dust adhesion force of the open-pit mine was tested under different factors using the abruption method. Each group of experiments was carried out three times, and the test results are shown in the Table 3.

Table 2 Factor-level settings

Level	Factors			
	Temperature T (℃)	Humidity RH/(%)	Particle size d_p(μm)	Pressure P (kPa)
1	25	50	22	12.48
2	30	60	30	24.79
3	35	70	45	37.45
4	40	80	75	49.9

Based on 48 groups of orthogonal test data, a multiple regression method was used to establish the relationship between dust adhesion force of soil pavement and various factors. According to the previous analysis, the relationship between temperature, humidity, particle size and pressure and adhesion force is nonlinear. Hence, the empirical equation for the adhesion between temperature, humidity and other factors was established, as shown in Eq. (3).

$$p = a \cdot T^{a_1} \cdot RH^{a_2} \cdot d_{\mathrm{p}}^{a_3} \cdot P^{a_4} \tag{3}$$

Taking the logarithm of both sides of Eq. (3), the following equations can be obtained:

$$\log p = \log a + a_1 \log T + a_2 \log RH + a_3 \log d_{\mathrm{p}} + a_4 \log P \tag{4}$$

To facilitate the solution, let $y = \log p$, $a_0 = \log a$, $x_1 = \log T$, $x_2 = \log RH$, $x_3 = \log d_p$, $x_4 = \log P$, and substitute them into the Eq. (4), thus transforming it into a multivariate linear equation as shown in Eq. (5).

$$y = a_0 + a_1 x_1 + a_2 x_2 + a_3 x_3 + a_4 x_4 \tag{5}$$

According to Eq. (5), the results of the orthogonal experiment can be expressed as follows:

$$\begin{cases} y_1 = a_0 + a_1 x_{11} + a_2 x_{12} + a_3 x_{13} + a_4 x_{14} + \varepsilon_1 \\ y_2 = a_0 + a_1 x_{21} + a_2 x_{22} + a_3 x_{23} + a_4 x_{24} + \varepsilon_2 \\ \vdots \\ y_{47} = a_0 + a_1 x_{471} + a_2 x_{472} + a_3 x_{473} + a_4 x_{474} + \varepsilon_{47} \\ y_{48} = a_0 + a_1 x_{481} + a_2 x_{482} + a_3 x_{483} + a_4 x_{484} + \varepsilon_{48} \end{cases} \tag{6}$$

where $\varepsilon_1, \varepsilon_2, \varepsilon_3 \ldots \varepsilon_{48}$ are independent of each other. Afterwards, let

$$\boldsymbol{Y} = \begin{bmatrix} y_1 \\ y_2 \\ \vdots \\ y_{47} \\ y_{48} \end{bmatrix}, \quad \boldsymbol{X} = \begin{bmatrix} 1 & x_{11} & x_{12} & \cdots & x_{14} \\ 1 & x_{21} & x_{22} & \cdots & x_{24} \\ \vdots & \vdots & \vdots & \ldots & \vdots \\ 1 & x_{471} & x_{472} & \cdots & x_{474} \\ 1 & x_{481} & x_{482} & \cdots & x_{484} \end{bmatrix}, \quad \boldsymbol{\alpha} = \begin{bmatrix} a_0 \\ a_1 \\ a_2 \\ a_3 \\ a_4 \end{bmatrix}, \quad \boldsymbol{\varepsilon} = \begin{bmatrix} \varepsilon_1 \\ \varepsilon_2 \\ \vdots \\ \varepsilon_{47} \\ \varepsilon_{48} \end{bmatrix}$$

Table 3 Orthogonal experimental results

serial number	Temperature T (℃)	Humidity RH (%)	Particle size d_p(μm)	Pressure P (kPa)	Adhesion force p (mg/cm^2)	Standard deviation
1	25	50	22	12.48	196.04	16.29
2	25	60	30	24.79	44.90	11.87
3	25	70	45	37.45	1629.30	163.27
4	25	80	75	49.9	2101.82	176.36
5	30	50	30	37.45	2955.22	224.72
6	30	60	22	49.9	509.86	49.97
7	30	70	75	12.48	275.02	63.51
8	30	80	45	24.79	4645.51	224.79
9	35	50	45	49.9	11.80	1.81
10	35	60	75	37.45	197.04	46.84
11	35	70	22	24.79	262.93	14.89
12	35	80	30	12.48	699.96	59.60
13	40	50	75	24.79	15.83	6.16
14	40	60	45	12.48	17.30	6.57
15	40	70	30	49.9	104.28	12.20
16	40	80	22	37.45	643.34	26.10

According to the rules of matrix operations, the expression could be expressed as matrix operation, as shown in Eq. (7):

$$\boldsymbol{Y} = \boldsymbol{\alpha X} + \boldsymbol{\varepsilon} \tag{7}$$

Using the least squares method to estimate the parameters (i.e., a_0, a_1, a_2, a_3, a_4), the regression equation is:

$$\hat{y} = a_0 + a_1 x_1 + a_2 x_2 + a_3 x_3 + a_4 x_4 \tag{8}$$

a could be calculated by the following equation:

$$a = \left(\boldsymbol{X^T X}\right)^{-1} \boldsymbol{X^T Y} = \left(\begin{bmatrix} 1 & 1 & 1 & \cdots & 1 \\ x_{11} & x_{21} & x_{31} & \cdots & x_{481} \\ \vdots & \vdots & \vdots & \vdots & \vdots \\ x_{13} & x_{23} & x_{33} & \cdots & x_{483} \\ x_{14} & x_{24} & x_{34} & \cdots & x_{484} \end{bmatrix} \begin{bmatrix} 1 & x_{11} & x_{12} & \cdots & x_{14} \\ 1 & x_{21} & x_{22} & \cdots & x_{24} \\ \vdots & \vdots & \vdots & \vdots & \vdots \\ 1 & x_{471} & x_{472} & \cdots & x_{474} \\ 1 & x_{481} & x_{482} & \cdots & x_{484} \end{bmatrix} \right)^{-1} \begin{bmatrix} 1 & 1 & 1 & \cdots & 1 \\ x_{11} & x_{21} & x_{31} & \cdots & x_{481} \\ \vdots & \vdots & \vdots & \vdots & \vdots \\ x_{13} & x_{23} & x_{33} & \cdots & x_{483} \\ x_{14} & x_{24} & x_{34} & \cdots & x_{484} \end{bmatrix} \begin{bmatrix} y_1 \\ y_2 \\ y_3 \\ \vdots \\ y_{48} \end{bmatrix} \tag{9}$$

The coefficient a could be obtained by substituting the orthogonal experiment results into Eq. (9). The coefficient a is calculated as follows:

$$a = \begin{bmatrix} -0.892 \\ -4.705 \\ 5.746 \\ -0.523 \\ 0.581 \end{bmatrix} \tag{10}$$

Based on the above parameters, the model of dust adhesion force of soil pavement of open-pit mine could be obtained as follows:

$$p = 10^{-0.892} \cdot T^{-4.705} \cdot RH^{5.746} \cdot d_p^{-0.523} \cdot P^{0.581} \tag{11}$$

In order to verify the accuracy of the established model, several groups of experimental values were selected for comparison with the predicted values, and the comparison results are shown in the Fig. 12. It is obvious that the model has excellent predictions for some results with errors within 15%, but there are also some large errors, such as the shaded area in the Fig. 12. Therefore, the accuracy of the model needs to be further improved, so Eq. (11) is written as:

$$p \propto T^{-4.705} \cdot RH^{5.746} \cdot d_p^{-0.523} \cdot P^{0.581}$$

Despite the dust adhesion force of soil pavement on open-pit mine is quantified in current work, the dust adhesion force is easily affected by its own physical and chemical characteristics, and the adhesion force of road dust varies from one mine site to another. Studying the adhesion force of soil pavement is important for the mechanism of road dust generation and the development of corresponding dust suppressants. Therefore, it is recommended to discuss dust adhesion force in future road dust control studies to develop an efficient dust suppressant.

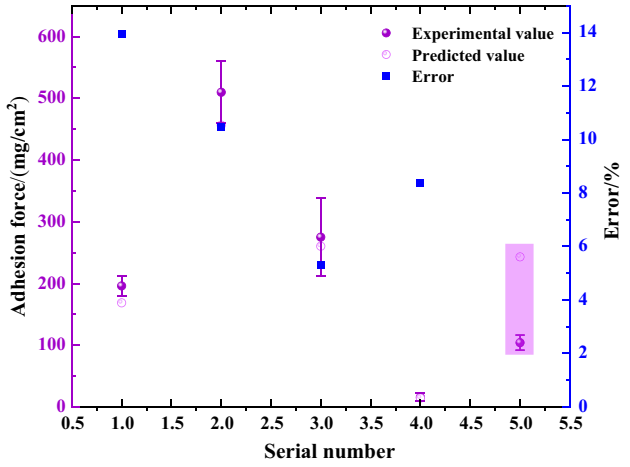

Fig. 12 Comparison between predicted value and experimental value

4 Conclusions

In this study, the dust microstructure and adhesion force of open-pit mine soil pavement were investigated by scanning electron microscopy, BET and abruption methods, and the following conclusions were drawn:

(1) The soil pavement dust of open-pit mine is mainly irregular quadrilateral, pentagonal and nearly circular. Besides, the adhesion force of the full-size dust with particle size is 8.09 mg/cm^2.

(2) The dust adhesion force decreases with the increase of dust particle size. When the dust particle size increased from 22 to 30 μm, the dust adhesion force decreases from 440.17 mg/cm^2 to 151.88 mg/cm^2. The dust adhesion force of the soil pavement of open-pit mine decreases with the increase of temperature. The dust adhesion force tended to be stable with temperature and was almost independent of temperature with the change of temperature and hardly affected by temperature when the temperature was greater than 30 ℃.

(3) With the increase of ambient humidity, the dust adhesion force of soil pavement of open-pit mine increases. When the humidity was more than 70%, the dust adhesion force could reach 2000 mg/cm^2. The dust adhesion force of soil pavement of open-pit mine increases gradually as the pressure increased. In addition, the increase trend of dust adhesion force is obvious when the pressure exceeded 24.79 kPa.

(4) A multiple regression method was employed to establish the dust adhesion force model for the soil pavement of open-pit mine, but the accuracy of the model needs to be further improved.

Author contribution JW: Conceptualization, Methodology, Data curation, Writing-Original draft preparation. CD: Supervision, Methodology, Writing-Reviewing. YW: Data curation. ZC: Data curation.

Funding National Key Research and Development Program of China (2022YFC2905003).

References

Barone TL, Hesse E, Seaman CE, Baran AJ, Beck TW, Harris ML, Jaques PA, Lee T, Mischler SE (2019) Calibration of the cloud and aerosol spectrometer for coal dust composition and morphology. Adv Powder Technol 30(9):1805–1814

Bucko MS, Magiera T, Johanson B, Petrovsky E, Pesonen LJ (2011) Identification of magnetic particulates in road dust accumulated on roadside snow using magnetic, geochemical and micro-morphological analyses. Environ Pollut 159(5):1266–1276

Chen P, Tang XY (2001) The research on the adsorption of nitrogen in low temperature and micro-pore properties in coal. J China Coal Soc 5:552–556 (**[in Chinese]**)

Deng T, Garg V, Bradley MSA (2021) A study of particle adhesion for cohesive powders using a novel mechanical surface energy tester. Powder Technol 391:46–56

(GB/T 16913–2008), China National Standard Press, Beijing, 2008.

Hu B, Freihaut JD, Bahnfleth WP, Thran B (2008) Measurements and factorial analysis of micron-sized particle adhesion force to indoor flooring materials by electrostatic detachment method. Aerosol Sci Technol 42(7):513–520

Isaifan RJ, Johnson D, Ackermann L, Figgis B, Ayou M (2019) Evaluation of the adhesion forces between dust particles and photovoltaic module surfaces. Sol Energy Mater Sol Cells 191:413–421

Jin L, Liu J, Guo J, Wang J, Wang T (2021) Physicochemical factors affecting the wettability of copper mine blasting dust. Int J Coal Sci Technol 8:265–273

Jaiswal RP, Kumar G, Kilroy CM, Beaudoin SP (2009) Modeling and validation of the van der Waals force during the adhesion of nanoscale objects to rough surfaces: a detailed description. Langmuir 25(18):10612–10623

Jayarathne A, Mummullage S, Gunawardana C, Egodawatta P, Ayoko GA, Goonetilleke A (2019) Influence of physicochemical properties of road dust on the build-up of hydrocarbons. Sci Total Environ 694:133812

Jones R, Pollock HM, Cleaver JAS, Hodges CS (2002) Adhesion forces between glass and silicon surfaces in air studied by AFM: effects of relative humidity, particle size, roughness, and surface treatment. Langmuir 18(21):8045–8055

Karde V, Dixit D, Ghoroi C (2017) Adhesion force approximation at varying consolidation stresses for fine powder under humid conditions. Adv Powder Technol 28(2):346–355

Klockner P, Seiwert B, Weyrauch S, Escher BI, Reemtsma T, Wagner S (2021) Comprehensive characterization of tire and road wear particles in highway tunnel road dust by use of size and density fractionation. Chemosphere 279:130530

Liu Y, Liu G, Yousaf B, Zhou C, Shen X (2021) Identification of the featured-element in fine road dust of cities with coal contamination by geochemical investigation and isotopic monitoring. Environ Int 152:106499

Mazzoli A, Favoni O (2012) Particle size, size distribution and morphological evaluation of airborne dust particles of diverse woods by Scanning Electron Microscopy and image processing program. Powder Technol 225:65–71

Nguyen TT, Rambanapasi C, de Boer AH, Frijlink HW, Ven PMVD, de Vries J, Busscher HJ, Maarschalk KVDV (2010) A centrifuge method to measure particle cohesion forces to substrate surfaces: the use of a force distribution concept for data interpretation. Int J Pharm 393(1–2):88–95

Qian J, Liu Z, Lin S, Li X, Ali M (2020) Study on microstructure characteristics of material evidence in coal dust explosion and its significance in accident investigation. Fuel 265:116992

Ramirez O, da Boit K, Blanco E, Silva LFO (2020) Hazardous thoracic and ultrafine particles from road dust in a Caribbean industrial city. Urban Climate 33:100655

Ripperger S, Hein K (2005) Measurement of adhesion forces in air with the vibration method. China Part 3(1):3–9

Shi Y, Ma Z, Chu D, Wang X, Sun F, Guo Z (2017) An experimental study of ash particles adhesion force in flue gas. Adv Powder Technol 28(6):1435–1442

Wiseman CLS, Levesque C, Rasmussen PE (2021) Characterizing the sources, concentrations and resuspension potential of metals and metalloids in the thoracic fraction of urban road dust. Sci Total Environ 786:147467

Yang H-H, Dhital NB, Wang L-C, Hsieh Y-S, Lee K-T, Hsu Y-T, Huang S-C (2019) Chemical characterization of fine particulate matter in gasoline and diesel vehicle exhaust. Aerosol Air Qual Res 19(6):1439–1449

Yan JM, Zhang PY (1979) Adsorption and coagulation. Science Press, Beijing (**[in Chinese]**)

Zafar U, Hare C, Hassanpour A, Ghadiri M (2014) Drop test: a new method to measure the particle adhesion force. Powder Technol 264:236–241

Zhang Y, Xing Y, Ding S, Cao Y, Gui X (2020) New method to measure interaction force between particle and air bubble/water droplet using a micro-Newton mechanics testing instrument. Powder Technol 373:142–146